

The COVID-19 vaccination campaign in Switzerland and its impact on disease spread

M. Bekker-Nielsen Dunbar and L. Held

Epidemiology, Biostatistics and Prevention Institute, University of Zurich

E-mail: maria.dunbar@uzh.ch

1

2 We analyse infectious disease case surveillance data stratified by region and
3 age group to estimate COVID-19 spread and gain an understanding of the
4 impact of introducing vaccines to counter the disease in Switzerland. The data
5 used in this work is extensive and detailed and includes information on weekly
6 number of cases and vaccination rates by age and region. Our approach takes
7 into account waning immunity. The statistical analysis allows us to determine
8 the effects of choosing alternative vaccination strategies. Our results indicate
9 greater uptake of vaccine would have led to fewer cases with a particularly
10 large effect on undervaccinated regions while an alternative distribution scheme
11 ignoring age would affect the vulnerable population at the time (the elderly)
12 and is less ideal.

13 **Keywords:** Vaccination coverage, infectious disease surveillance, endemic-epidemic mod-
14 elling, coronavirus disease 2019 (COVID-19)

15

16 1 Introduction

17 Each year vaccines (pre-exposure pharmaceutical prophylaxis interventions) save lives
18 by reducing preventable illness and death. Though vaccines are tested vigorously to en-
19 sure they are efficacious and monitored extensively to ensure they are effective and safe,

20 they are underutilised in routine immunisation. This has led to outbreaks of vaccine-
21 preventable diseases that were previously eliminated in Europe, such as measles [1]. There
22 is a concern that newly developed vaccines in response to pandemics will not be accepted
23 by the population they seek to protect.

24 In December 2020, vaccines to prevent severe acute respiratory syndrome coronavirus
25 2 (SARS-CoV-2, the causative agent of COVID-19) infections were authorised for use in
26 Switzerland. They were distributed in 2021 following an age-based distribution scheme
27 going from oldest to youngest. A booster (additional dose of vaccine after immunity is
28 achieved which is used to maintain immunity) was included in the immunisation schedule
29 for COVID-19 late in 2021 and continued during 2022 following the same age-based distri-
30 bution scheme. As those aged 65 years and older were first invited to be immunised, later
31 followed by 16 to 64 year olds, and finally 12 to 15 year olds, changes in the age profile of
32 cases (who is getting sick) have been observed. Additionally, in Switzerland, changes in
33 the spatial distribution of cases (where people are getting sick) have also been observed,
34 with a shift from urban centres to more rural, unvaccinated communities.

35 Vaccine hesitancy (defined as a delay in acceptance or refusal of vaccines despite avail-
36 ability) is found in Switzerland, where vaccination is not mandatory. This is a current issue
37 of mounting concern that needs to be solved. The World Health Organization named vac-
38 cine hesitancy as one of the ten threats to global health already in 2019, noting its detri-
39 mental effects on populations who are less protected against life-threatening diseases even
40 in non-pandemic settings. Vaccine hesitancy affects the uptake of vaccines and likely also
41 the adherence to other public health interventions in certain population groups. An un-
42 dervaccinated population has the potential to hamper disease control efforts for the entire
43 country. Others have noted that in the Swiss context “vaccine hesitancy and underimmu-
44 nisation seem to be specific to certain population subgroups” [2]. COVID-19 is currently
45 the only human coronavirus for which there is a vaccine available but hesitancy persists [3].
46 Ongoing work seeks to understand the drivers of Swiss vaccine hesitancy [4].

47 We study COVID-19 incidence data from 2021 (from 1st January 2021 to 30th Novem-
48 ber 2021, both dates included) to examine the effect of vaccines on the spread of disease

49 in Switzerland. We analyse weekly cases in two separate analyses, one is stratified by age
50 group and one is stratified by region. This approach is motivated by cases being observed
51 among younger ages in this time period (compared with earlier), with cases also exhibiting
52 spatial heterogeneity in regions, as well as vaccination rates differing by unit (age group or
53 region). Switzerland provides a unique opportunity to examine the effects of vaccination
54 heterogeneity due to its federalised nature. Regions are less harmonised than in other Eu-
55 ropean countries. We seek to determine the impact of the current vaccination strategy and
56 the effect of regions with low vaccine uptake.

57 Using epidemic data sources from infectious disease surveillance systems at weekly
58 resolution, we are able to capture the spread of disease across space and between age
59 groups through an endemic-epidemic modelling approach. The vaccination coverage is
60 time-dependent, age group-dependent, and region-dependent. Our approach builds upon
61 a unique incorporation of time-varying vaccination coverage in an endemic-epidemic model
62 with time-varying transmission weights. Time-varying transmission weights reflecting weekly
63 levels of situational measures (amount of disease control) is a novel inclusion in the model
64 since the advent of COVID-19, which has proven to be useful in examining policy questions
65 [5–7]. Outlined here is a wider application which also includes vaccination effects. We in-
66 vite interested readers to our study protocol [8] which contains even more detail.

67 Vaccination coverage has previously been included in endemic-epidemic modelling [9–
68 12] for routine immunisation without taking into account changes over time (assuming
69 stationarity). We include vaccination coverage in a similar manner in our models; to our
70 knowledge the first endemic-epidemic model for COVID-19 which includes time and unit-
71 specific vaccination rates. Calls for other vaccination distribution criteria than age to be
72 considered when introducing novel vaccines to immunisation schedules in pandemic set-
73 tings, such as socio-economic status [13], have been made. For this reason, we analyse
74 alternative scenarios (an approach which has successfully been utilised in the analysis of
75 non-pharmaceutical interventions to evaluate the impact of their timing [5–7]) to examine
76 other rollout strategy schemes and uptake options (increased coverage).

77 2 Material

78 The data considered in this work includes temporal variables (week of reporting or
79 recording/entry), biological variables (number of cases, age of case, dose-specific vac-
80 cination information), and spatial variables (region). Data is publicly available from the
81 Swiss public health authority's COVID-19-specific website (BAG) www.covid19.admin.ch
82 and introduced in our study protocol [8]. Auxiliary data is provided by Mistry et al. [14]
83 (contacts), Hale et al. [15] (policy), and Data for Good¹ (mobility) and where merging of
84 data is necessary, the groupings and temporal resolution used in the data from BAG are
85 matched. The age bands provided are ten year age bands, however we have not included
86 the age group 0 – 9 in this work as the focus is on the protective effect of vaccines and
87 they received none during the study period leading to a vaccination coverage which is con-
88 stantly zero, providing no information to the model.

89 2.1 Spatial dispersion

90 Spatial dispersion is included in the model to reflect how disease spreads. Switzerland
91 consists of 26 regions (Figure 2). The adjacencies between the 26 Swiss regions are given
92 in a matrix of neighbourhood order $\mathbf{o} = (o_{rr'})$ denoting the distance from one region r to
93 another r' (Figure 2). In this calculation, we decided that Neuchâtel (NE) and Jura (JU)
94 as well as Schaffhausen (SH) and Thurgau (TG) do not share a border as when looking at
95 a regular map they did not share most of their border in common.

96 To reflect additional changes in movement during the study period as a result of dis-
97 ease control policy implemented, we include mobility data m_{rt} (Figure 1) measuring the
98 average change in mobility in region r in week t . The data is provided as a change from
99 baseline (February 2020) which we normalise by transforming it by $\frac{x - \min(x)}{\max(x) - \min(x)}$ to ensure
100 that we do not have negative transmission weights in our model (as the change from base-
101 line is sometimes given as a negative value). Mobility data was not available for Appen-
102 zell Innerrhoden (AI) so we imputed them with values from the adjoining region Appenzell

¹Use of this data is not an endorsement of Facebook/Meta

103 Ausserhoden (AR).

The adjacency matrix is adjusted by mobility data like in Grimée et al. [5] such that we obtain time-varying adjacency matrices w (short form for adjacency matrices at each time point t) with entries:

$$w_{r,r',t} = \frac{1}{(o_{rr'} + 1)} \cdot m_{rt} \quad (1)$$

104 (Figure 3). We see an increase in mobility during the middle of the study period (Figure 1).

105 This means we will expect to observe increased transmission opportunities in certain re-
106 gions during that time.

107 2.2 Contacts

Respiratory diseases such as COVID-19 are transmitted through contact between age group a and a' . We incorporate a contact matrix $c = (c_{aa'})$ in the model to reflect the pattern of spread of the disease across age groups. The Swiss contact matrices from Mistry et al. [14] (Figure 2) are used in this work and aggregated to the ten year age bands used in the case data. Contacts occur in four locations l (household, school, work, and other). The contact matrices are adjusted by the policy data like in Bekker-Nielsen Dunbar et al. [6, 7] such that we obtain time-varying contact matrices w for each week t across all locations l with entries given by:

$$w_{a,a',t} = m_t \cdot \sum_l q_{lt} \cdot c_{a,a',l} \quad (2)$$

108 where the proportionality factor $q_{lt} = q_l \cdot q_t$ is informed by q_l which is a weight for con-
109 tacts in location l (which is provided with the location-specific contact matrices) and q_t
110 which denotes policy implemented in week t (Figure 3). Once we have calculated the to-
111 tal contacts using this factor, we additionally incorporate the average change in mobility
112 across regions in week t , m_t (Figure 1) across all contacts because the policy indicators q_t
113 do not capture more nuanced changes in transmission opportunities such as those caused
114 by public holidays whereas the mobility data is expected to encapsulate such aspects. The
115 mobility m_{rt} is averaged over regions to obtain m_t . Earlier policy data was more granular.
116 We divide the raw policy indicators by the maximum level it can take and then impose a

117 lower bound of 0.001 to obtain q_t (the lower bound reflects that some contacts still oc-
118 cur when measures are in place). As in Bekker-Nielsen Dunbar et al. [6, 7] $q_t \equiv 1$ in the
119 household setting.

120 2.3 Vaccines

The vaccination coverage is calculated based on the second (full immunity) and third doses (“booster”) of the vaccine as

$$x_{it} = \sum_{s \leq t} u(t-s) \left(x_{is}^{(2)} + x_{is}^{(3)} \right) \quad (3)$$

121 where $x_{is}^{(d)}$ is the vaccination coverage of dose d ($d = 2, 3$) for unit i in week s (doses
122 given at time s scaled by the population of unit i), week s occurs before week t , and $u(\cdot)$
123 is the waning function (Figure 4). We apply the waning function $u(\cdot)$ to account for wan-
124 ing immunity in our vaccination coverage calculation (see the supporting information (file
125 sens) for a sensitivity analysis of $u(\cdot)$). The unit i can either be age groups (a) or regions
126 (r). This approach allows us to determine the vaccination coverage in each week t taking
127 into account that the COVID-19 vaccines do not provide lifelong immunity. For each unit
128 at each time point, the cumulative doses given are the sum of vaccines given in that week
129 as well as the waned vaccines given in previous weeks t . The vaccination coverage is shown
130 in Figure 5.

131 3 Methods

132 We fit four types of endemic-epidemic models using the open source software package
133 developed by Meyer et al. [17]. The endemic-epidemic model is a time series-based mod-
134 elling approach for infectious disease surveillance first formulated in Held et al. [18]. Since
135 its introduction it has been extended to include vaccination coverage [9], random inter-
136 cepts [19], seasonal effects [20], time-constant transmission weights between units relaxing
137 a homogenous mixing assumption [21, 22], prediction and forecasting [23], and most re-
138 cently time-varying transmission weights [5–7].

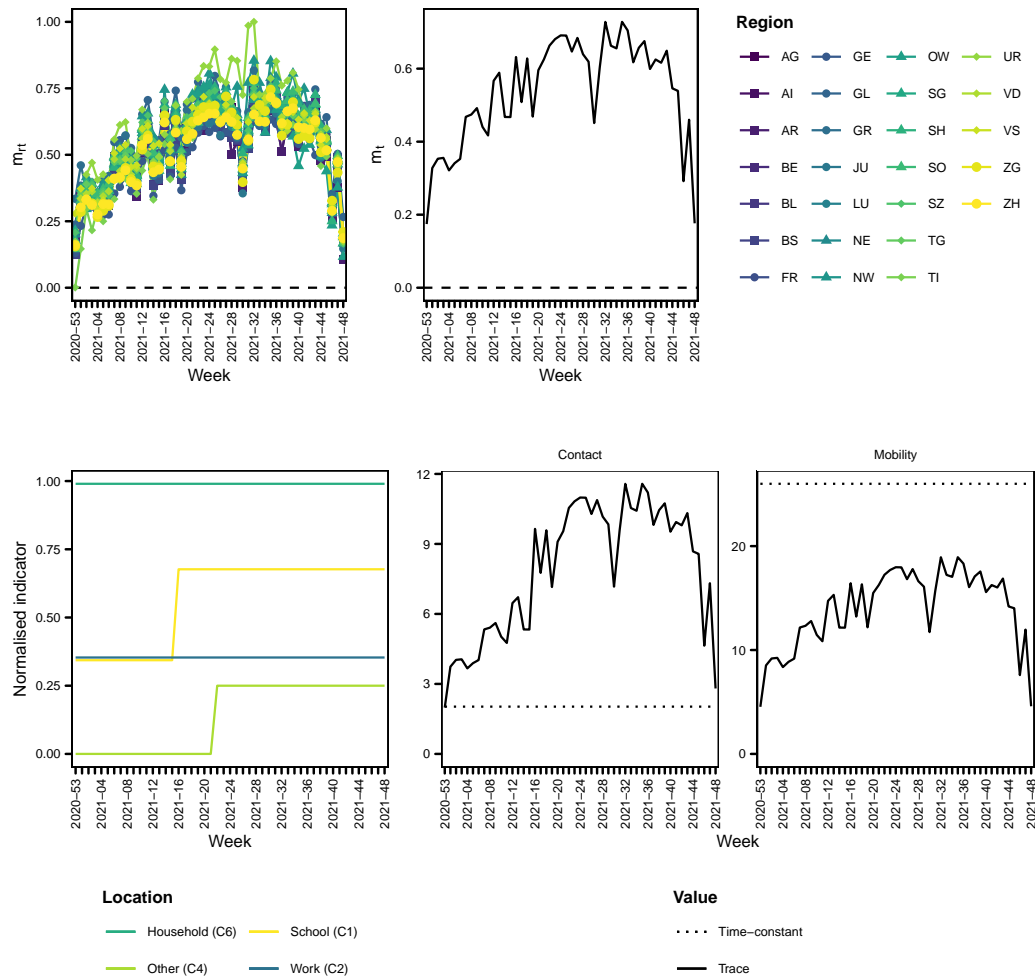


Figure 1: Mobility m_{rt} (above left) and m_t (above right), policy q_t (bottom left), and the trace (sum of the diagonal) of the contact matrix (bottom middle) and adjacency matrix (bottom right) at each time compared with the trace of the equivalent unadjusted hence time-constant transmission weights matrix (dashed lines). The abbreviations for regions are listed in the supporting information (file supp)

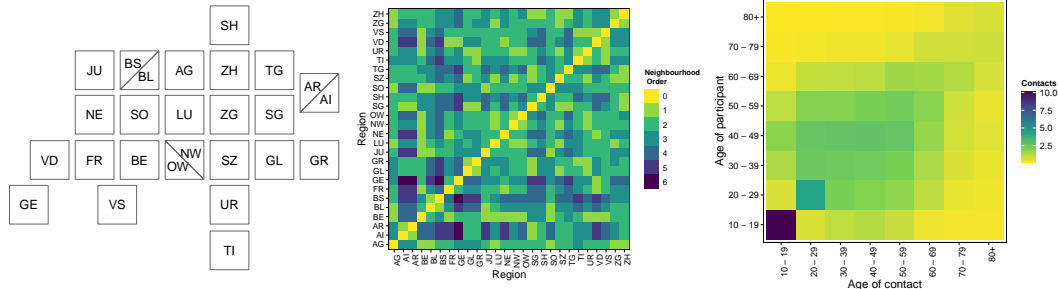


Figure 2: Swiss regions presented as map tiles (left; source: EBG [16]), adjacencies between the regions $\mathbf{o} = (o_{rr'})$ (middle), and contacts between age groups in Switzerland $\mathbf{c} = (c_{aa'})$ (right)

139 We chose which effects to include in our model on the basis of scoping the literature
 140 for other endemic-epidemic models with vaccination coverage (Table 1). The inclusion of
 141 previous season's incidence does not make sense for emerging infectious disease such as
 142 COVID-19 as the situation is ever-changing.

143 3.1 Model

The endemic-epidemic model is given by

$$Y_{it} \mid Y_{i,t-1} \sim \text{NegBin}(\lambda_{it}, \psi) \quad (4)$$

$$\lambda_{it} = \underbrace{\nu_{it} f_i}_{\text{endemic}} + \underbrace{\phi_{it} \sum_{i'} w_{i,i',t} Y_{i',t-1}}_{\text{epidemic}} \quad (5)$$

144 Cases Y_{it} observed in week t in unit i are conditionally negative binomially distributed
 145 with by mean λ and overdispersion ψ (4). The unit i can either be age groups (a) or re-
 146 gions (r). The mean of the negative binomial distribution λ is additively decomposed into
 147 an endemic component with log-linear predictor ν and an epidemic component with log-
 148 linear predictor ϕ (5). Previous cases $Y_{i,t-1}$ in all units are weighted by the transmission
 149 weights $w_{i,i',t}$ and the population fraction f_i (given as the size of the population for unit i
 150 compared with the total population) enters as an offset in the endemic component.

We name our four types of endemic-epidemic models based on the components where

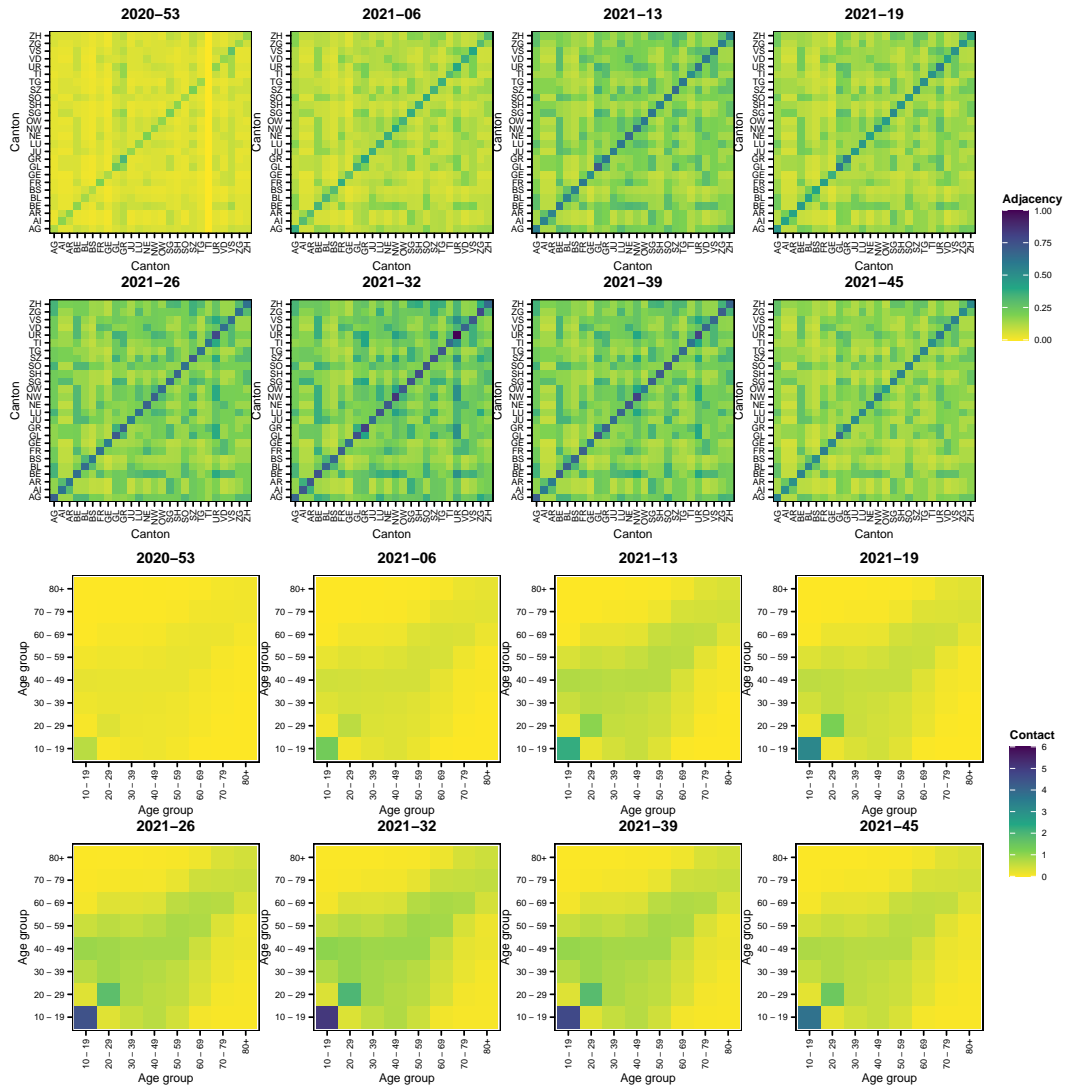


Figure 3: Snapshot of time-varying adjacency matrices w (above) and snapshot of time-varying contact matrices w (below), see the supporting information (file supp) for the full sets

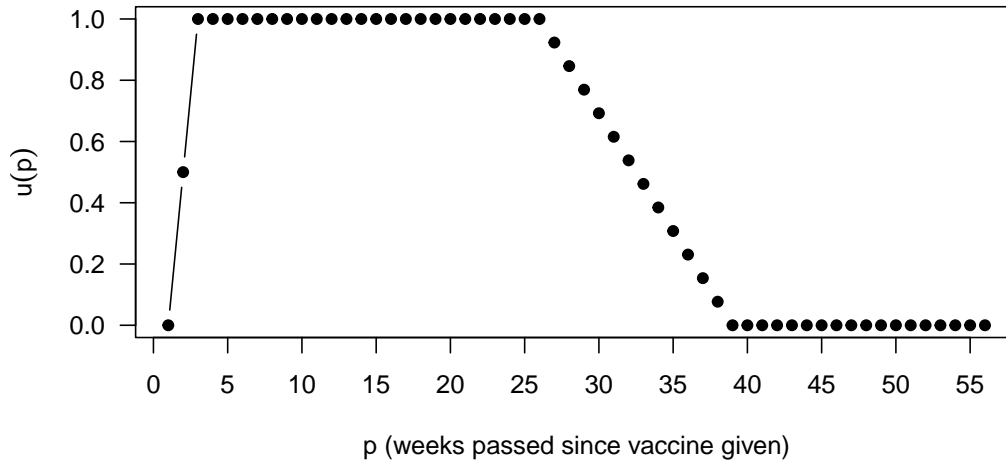


Figure 4: Waning function $u(p)$ used in calculation of (3). Adapted from Bekker-Nielsen Dunbar and Held [8]

the vaccination coverage is included. We consider the following four combinations of log-linear predictors ν and ϕ

$$\log(\nu_{it}) = \alpha_i^{(\nu)} + \gamma^{(\nu)\top} \mathbf{z}_{it}^{(\nu)} \quad (\text{Neither})$$

$$\log(\phi_{it}) = \alpha_i^{(\phi)} + \gamma^{(\phi)\top} \mathbf{z}_{it}^{(\phi)}$$

$$\log(\nu_{it}) = \alpha_i^{(\nu)} + \beta^{(\nu)} \log(1 - x_{it}) + \gamma^{(\nu)\top} \mathbf{z}_{it}^{(\nu)} \quad (\text{Endemic})$$

$$\log(\phi_{it}) = \alpha_i^{(\phi)} + \gamma^{(\phi)\top} \mathbf{z}_{it}^{(\phi)}$$

$$\log(\nu_{it}) = \alpha_i^{(\nu)} + \gamma^{(\nu)\top} \mathbf{z}_{it}^{(\nu)} \quad (\text{Epidemic})$$

$$\log(\phi_{it}) = \alpha_i^{(\phi)} + \beta^{(\phi)} \log(1 - x_{it}) + \gamma^{(\phi)\top} \mathbf{z}_{it}^{(\phi)}$$

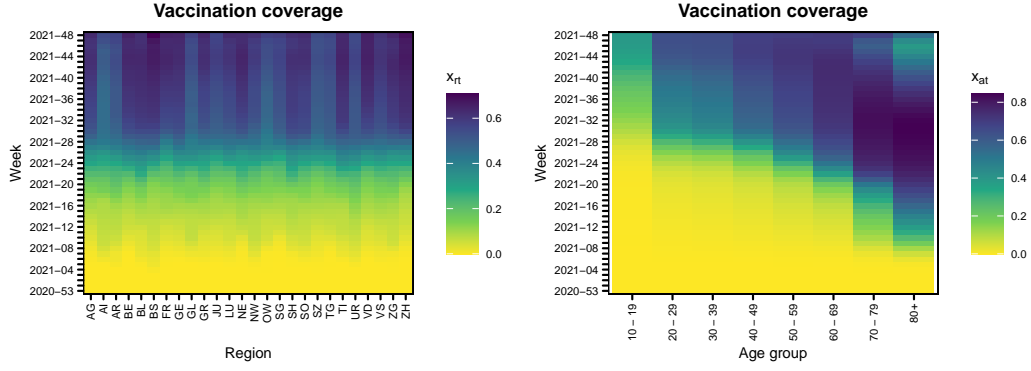


Figure 5: Calculated vaccination coverage taking into account waning immunity x_{it} by region (left) and age group (right). The time scale goes from bottom to top

$$\begin{aligned}\log(\nu_{it}) &= \alpha_i^{(\nu)} + \beta^{(\nu)} \log(1 - x_{it}) + \gamma^{(\nu)\top} \mathbf{z}_{it}^{(\nu)} & (\text{Both}) \\ \log(\phi_{it}) &= \alpha_i^{(\phi)} + \beta^{(\phi)} \log(1 - x_{it}) + \gamma^{(\phi)\top} \mathbf{z}_{it}^{(\phi)}\end{aligned}$$

151 We use the log-proportion of the unvaccinated population as suggested by Herzog
152 et al. [9] and used by other endemic-epidemic models in the literature (Table 1). Thus the
153 log-transformed vaccination coverage $\log(1 - x_{it})$ enters the model as a coefficient in the
154 log-linear predictors. Additional effects enter as either fixed or random effects [19] of unit
155 α (intercepts) or additional covariates \mathbf{z} . We consider

$$\gamma^{(\nu)\top} \mathbf{z}_{it}^{(\nu)} = \gamma_{\sin}^{\nu} \sin\left(\frac{2\pi t}{52}\right) + \gamma_{\cos}^{\nu} \cos\left(\frac{2\pi t}{52}\right) + \gamma_{\text{time}}^{\nu} (t - \tilde{t}), \quad i = a, r \quad (6)$$

$$\gamma^{(\phi)\top} \mathbf{z}_{at}^{(\phi)} = \gamma_{\sin}^{\phi} \sin\left(\frac{2\pi t}{52}\right) + \gamma_{\cos}^{\phi} \cos\left(\frac{2\pi t}{52}\right) + \gamma_{\text{time}}^{\phi} (t - \tilde{t}) \quad (7)$$

$$\gamma^{(\phi)\top} \mathbf{z}_{rt}^{(\phi)} = \gamma_{\sin}^{\phi} \sin\left(\frac{2\pi t}{52}\right) + \gamma_{\cos}^{\phi} \cos\left(\frac{2\pi t}{52}\right) + \gamma_{\text{time}}^{\phi} (t - \tilde{t}) + \gamma_{\text{gravity}}^{\phi} \log(P_r) \quad (8)$$

156 where we have included a sine-cosine wave to account for yearly (52 weeks) oscillation
157 [20], \tilde{t} denotes the median of the study period (the time trend is centered to make it more
158 stable and is intended to capture fluctuations not captured by the sine-cosine wave) and
159 $\log(P_r)$ is the log population count of region r . The latter is known as the gravity model

160 [24] and reflects the fact that a greater attraction (higher mass) is to be expected from
161 populous regions. We fit models to regional units r and age group units a separately.

162 While ours is the first endemic-epidemic model for COVID-19 with time-varying vacci-
163 nation coverage at weekly granularity, previous models have been constructed for measles
164 with vaccination coverage [9–12] (Table 1). While other research groups [9–12] considered
165 a different disease (measles) and setting (non-pandemic), their estimated effects of vacci-
166 nation coverage are included in Figure 8 as a comparison with our work. We estimate the
167 effect of vaccination coverage for models with time constant transmission weights to allow
168 for such that we can liken the results for novel vaccines with routine scheduled immuni-
169 sation. We then focus on the results for models with time-varying transmission weights
170 $\mathbf{w} = (w_{ii't})$ as a constant transmission weight matrix $\mathbf{w} = (w_{ii'})$ is not informative for a
171 situation with as many changes as expected in the setting considered; an emerging infec-
172 tious disease with the introduction of a pharmaceutical countermeasure.

173 3.2 Scenario prediction

174 We predict the number of expected COVID-19 cases under the alternative scenarios of
175 vaccination distribution hence coverage. Using the multivariate path forecasting method
176 from Held et al. [23, Appendix A] we predict the mean (first moment) incidence by unit
177 (age group or region). The single-step prediction approach is iteratively applied to obtain
178 multivariate multi-step predictions. We use the estimated model coefficients in the predic-
179 tion approach rather than refitting the model.

180 In one scenario we replace the observed vaccination coverage covariate (Figure 5)
181 $\log(1 - x_{it})$ with an alternative option which for x_{rt} is the maximum vaccination coverage
182 in any region r (Figure 6) and for x_{at} is the number of vaccines given to each age group
183 a after redistributing the total vaccines given at any time to be given to all age groups
184 by amounts proportional to the size of the age group (see the supporting information (file
185 supp) for the redistribution). This scenario projection allows us to determine the expected
186 impact of two alternative vaccination distribution schemes.

187 In line with recommendations by den Boon et al. [25] we present results with within-

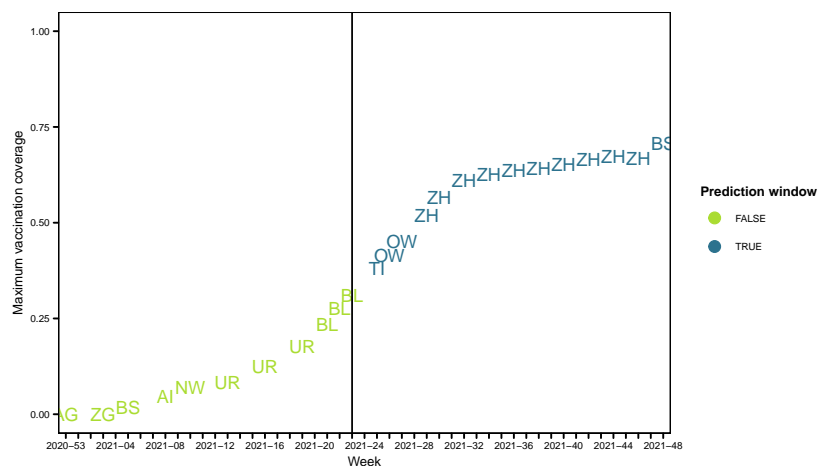


Figure 6: Overview of which region has the maximum vaccination coverage in a given week t providing the alternative uptake scenario we consider for regions. The vertical line denotes where our predictions begin

188 model uncertainty ranges. These are obtained by simulating the estimated coefficients (Ta-
 189 ble 4) from our fitted models assuming a multivariate normal distribution [like 5–7].

190 4 Results

191 We fit models to regional units r and age group units a separately. We provide here
 192 an overview of results and refer the interested reader to the supporting information (files
 193 `models-age` and `models-regions`) for full model results (there are results for in total 26
 194 regions and eight age groups). The models contain the effects outlined in Table 1. Our es-
 195 timated effect for vaccination coverage in a model with time constant transmission weights
 196 $\mathbf{w} = (w_{ii'})$ is in line with the results obtained by other research groups [9–12] (Table 2 and
 197 Figure 8). We now focus on the results for time-varying transmission weights $\mathbf{w} = (w_{ii't})$.

198 As some of the endemic effects had large confidence intervals when including just a
 199 simple intercept (intercept that was not unit-specific $\alpha^{(\cdot)}$), we included effects of unit (age
 200 group or region) $\alpha^{(\nu)}$ in the endemic component. This is one of the strategies outlined
 201 in Meyer et al. [26]. As we have a large number of units in our analysis of regions we de-
 202 cided to include a random intercept rather than a fixed intercept for this analysis. How-

Table 1: Comparison with the literature (measles) and effects included in our COVID-19 models

Effect	Measles				COVID-19	
	Herzog et al. [9]	Robert et al. [10]	Nguyen et al. [11]	Lu and Meyer [12]	Region	Age
Vaccination coverage	✓ ¹	✓ ²	✓ ¹	✓ ³	✓	✓
Sine-cosine wave	✓	✓	✓	✓	✓	✓
Population fraction offset in endemic component	✓	✓ ⁴	✓	✓	✓	✓
Intercepts	✓	✓	✓	✓	✓	✓
Random effects of unit			✓		✓	
Fixed effects of unit						✓
Centered time trend			✓ ⁵		✓	✓
Previous season's incidence		✓			NA	NA
Geographical size (surface area)		✓				
Gravity model in epidemic component		✓			✓	

1: constant, 2: averaged, 3: yearly, 4: is population count rather than fraction, 5: trend is not centered

203 ever, when using random effects, Akaike's information criterion can no longer be used for
 204 model selection and we elected instead to use the Dawid-Sebastani score (DSS) given in
 205 Held et al. [23]. We calculated the one-step-ahead score for the final observation date ISO
 206 week 2021-48 based on the predictions and observed data from the rest of the study pe-
 207 riod (ISO weeks 2020-53 to 2021-47). An overview of the different models is provided in
 208 Table 3. We see that the best fitting models with time-varying weights both have vaccina-
 209 tion coverage covariate in the endemic component.

210 We present results for the best fitting model (the model with vaccination coverage in
 211 the endemic component) for each unit (stratum defined by age group or region) type. We
 212 show the fitted values summed across units in Figure 7. while results for individual units
 213 are found in the supporting information (files `models-age` and `models-regions`). The
 214 models fit the data well and show similar patterns (Figure 7) with an increase in endemic
 215 cases in the summer and autumn (June to October; ISO weeks 2021-25 to 2021-40). We
 216 believe this to be a summer holiday effect as international travel increased after a year with
 217 many electing to have a "staycation" in 2020, so there is an increase in imported cases
 218 during this time.

Table 2: Vaccination coverage covariate estimates $\hat{\beta}$ and standard errors in brackets

Weight option		Neither	Endemic	Epidemic	Both	
					Endemic	Epidemic
Region	Time-constant (1R)	–	4.401 (1.343)	3.251 (0.216)	1.677 (1.038)	3.206 (0.216)
	Time-varying (2R)	–	3.312 (1.035)	2.688 (0.201)	1.739 (0.846)	2.642 (0.2)
Age	Time-constant (1A)	–	2.042 (0.246)	0.722 (0.062)	2.118 (0.14)	0.422 (0.055)
	Time-varying (2A)	–	2.234 (0.121)	0.578 (0.07)	2.033 (0.116)	0.238 (0.059)

Table 3: Endemic-epidemic models and goodness of fit (the lowest Dawid-Sebastani score (DSS) values for the models with time-varying transmission weights are marked in bold)

Transmission weights	Model	DSS	
		Region	Age
Time-constant	neither	15.25	18.57
Time-constant	endemic	15.34	20.59
Time-constant	epidemic	15.24	16.08
Time-constant	both	15.24	18.6
Time-varying	neither	13.79	21.22
Time-varying	endemic	13.74	18.45
Time-varying	epidemic	17.08	23.9
Time-varying	both	16.99	19.61

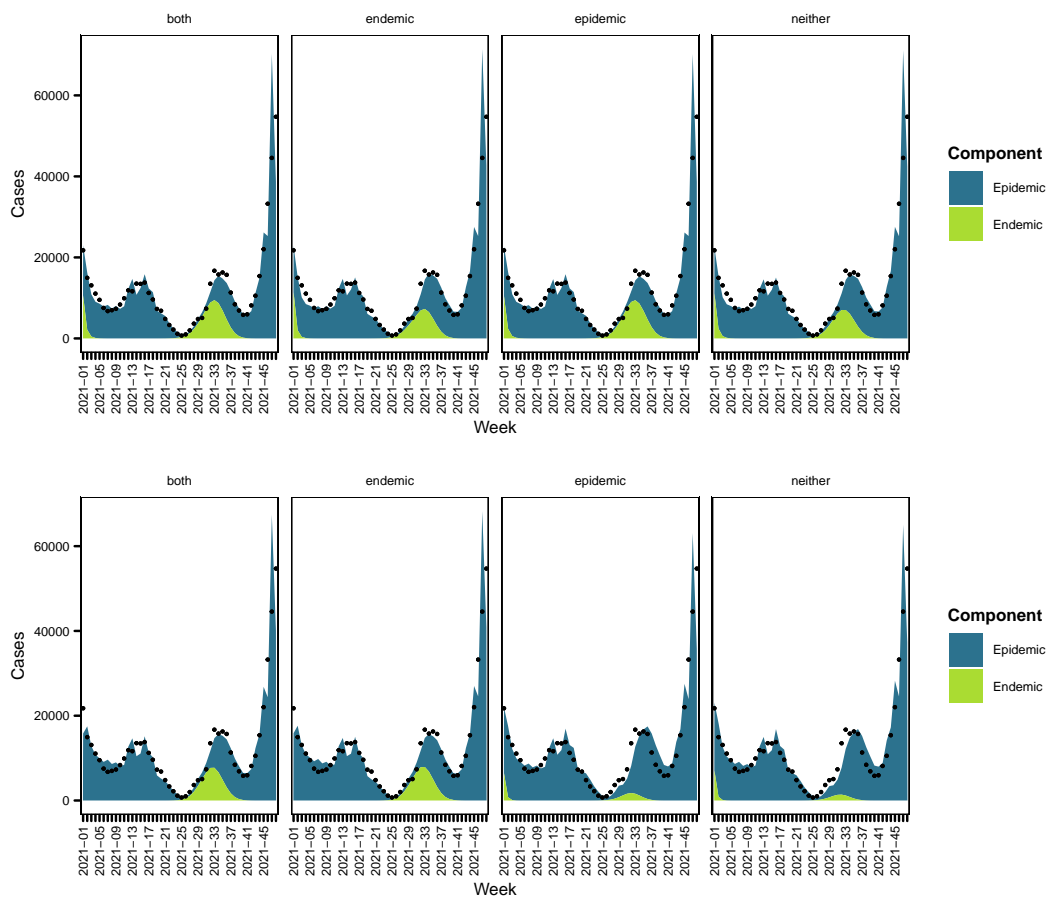


Figure 7: Model fits for models with time-varying transmission weights with region (above) and age groups (below)

219 4.1 Spatial dispersion

220 The model estimates for the models with time-varying transmission weights (Table 4)
221 show a greater effect of vaccination coverage (β) in the epidemic component $\beta^{(\nu)}$ than
222 the endemic component $\beta^{(\phi)}$ when both are included in the models for regions. The ran-
223 dom effects for region are greater for the large regions (Geneva/GE, Basel/BS and BL,
224 Zug/ZH, and Zurich/ZH) in the endemic component (Figure 9). Bordering regions Ticino
225 (TI), Geneva (GE), Basel (BS and BL) and Schaffhausen (SH) have smaller effects in the
226 epidemic component which may be due to cross-border medical seeking behaviour. The
227 gravity model is included in the region-based model. The effect is positive indicating that
228 there is more influx from larger populations (urban centres) and so we would expect to
229 see more cases in such regions. It seems stable across models considered. The linear time
230 trend does not seem to contribute much, indicating the yearly-duration sine-cosine waves
231 may capture most of the fluctuation. The sine-cosine waves are most similar in the epi-
232 demic component ($\gamma_{\sin}^{(\phi)}$ and $\gamma_{\sin}^{(\nu)}$), which is more pronounced for the model with regions.
233 The overdispersion ψ is largest for the model without vaccination coverage but is similar
234 for the model selected.

235 4.2 Contacts

236 There is a greater effect of vaccination coverage (β) in the epidemic component $\beta^{(\nu)}$
237 than the endemic component $\beta^{(\phi)}$ when both are included in the models for age group but
238 effect in the endemic component is much smaller than seen in the regional model in the
239 age group-based models with tighter confidence bands. There is no common pattern for
240 the fixed effect of age group $\alpha^{(\phi)}$ indicating that this could be an important effect to in-
241 clude. Such an effect was not included in the endemic component $\alpha^{(\nu)}$ due to convergence
242 issues. The sine-cosine waves are again rather stable in the epidemic component. The
243 overdispersion ψ is largest for the model without vaccination coverage but experiences a
244 greater decrease when this covariate is included for the models with age groups. The linear
245 time trend again does not seem to contribute much to the models.

Table 4: Model coefficient estimates for models with standard errors in brackets

	Region				Age			
	neither	endemic	epidemic	both	neither	endemic	epidemic	both
γ_{\sin}^{ϕ}	0.674 (0.04)	0.687 (0.039)	0.247 (0.049)	0.255 (0.049)	0.443 (0.053)	0.661 (0.042)	0.329 (0.051)	0.604 (0.044)
γ_{\cos}^{ϕ}	0.708 (0.023)	0.722 (0.023)	0.818 (0.024)	0.821 (0.024)	0.653 (0.034)	0.913 (0.028)	0.633 (0.03)	0.897 (0.028)
$\gamma_{\text{gravity}}^{\phi}$	0.779 (0.033)	0.782 (0.033)	0.838 (0.029)	0.838 (0.029)				
$\gamma_{\text{time}}^{\phi}$	0.036 (0.002)	0.036 (0.002)	0.085 (0.004)	0.084 (0.004)	0.018 (0.003)	0.024 (0.002)	0.029 (0.003)	0.028 (0.002)
$\alpha_{\text{region}}^{\phi}$	0.798 (0.131)	0.802 (0.13)	2.118 (0.15)	2.099 (0.15)				
γ_{\sin}^{ν}	-9.588 (0.564)	-11.467 (0.832)	-9.393 (0.425)	-10.438 (0.669)	-12.641 (0.531)	-8.225 (1.141)	-13.084 (0.427)	-8.334 (1.134)
γ_{\cos}^{ν}	-3.972 (0.402)	-4.586 (0.45)	-3.621 (0.281)	-4.004 (0.342)	-6.101 (0.337)	-7.185 (0.183)	-5.937 (0.27)	-7.127 (0.182)
$\gamma_{\text{time}}^{\nu}$	-0.48 (0.036)	-0.475 (0.035)	-0.446 (0.026)	-0.448 (0.026)	-0.715 (0.023)	-0.033 (0.105)	-0.706 (0.021)	-0.053 (0.105)
$\alpha_{\text{region}}^{\nu}$	3.208 (0.397)	4.092 (0.471)	3.575 (0.294)	3.982 (0.358)				
ψ	0.117 (0.005)	0.115 (0.005)	0.101 (0.005)	0.101 (0.005)	0.11 (0.008)	0.055 (0.004)	0.094 (0.007)	0.053 (0.004)
$\beta^{(\nu)}$		3.312 (1.035)		1.739 (0.846)		2.234 (0.121)		2.033 (0.116)
$\beta^{(\phi)}$			2.688 (0.201)	2.642 (0.2)			0.578 (0.07)	0.238 (0.059)
α_{10-19}^{ϕ}					-1.429 (0.051)	-1.681 (0.041)	-1.357 (0.048)	-1.625 (0.042)
α_{20-29}^{ϕ}					-0.931 (0.053)	-1.239 (0.042)	-0.753 (0.053)	-1.145 (0.047)
α_{30-39}^{ϕ}					-0.974 (0.053)	-1.167 (0.04)	-0.769 (0.054)	-1.073 (0.046)
α_{40-49}^{ϕ}					-1.296 (0.052)	-1.406 (0.039)	-1.031 (0.057)	-1.296 (0.047)
α_{50-59}^{ϕ}					-1.257 (0.053)	-1.338 (0.039)	-0.948 (0.061)	-1.215 (0.049)
α_{60-69}^{ϕ}					-1.449 (0.053)	-1.5 (0.039)	-1.082 (0.066)	-1.354 (0.053)
α_{70-79}^{ϕ}					-1.196 (0.054)	-1.21 (0.04)	-0.766 (0.072)	-1.04 (0.058)
α_{80+}^{ϕ}					-0.541 (0.054)	-0.535 (0.04)	-0.084 (0.077)	-0.358 (0.06)

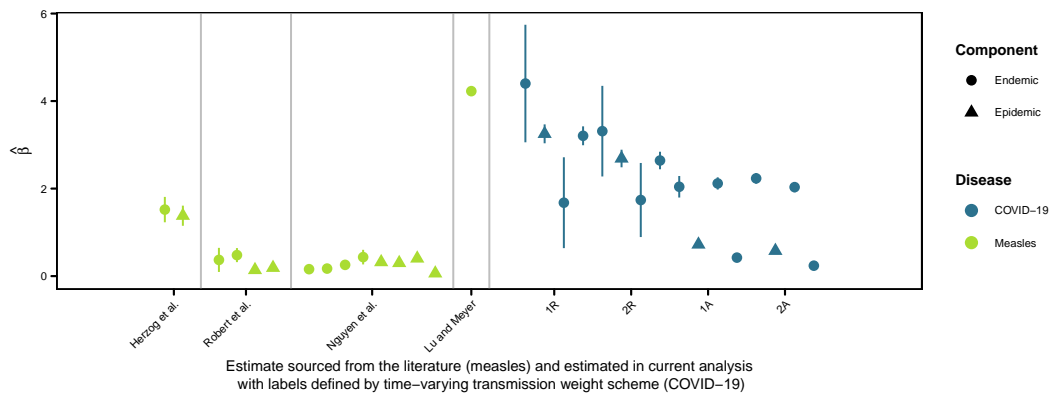


Figure 8: Overview of vaccination coverage estimates found in endemic-epidemic models. Labels for our models are provided in Table 2

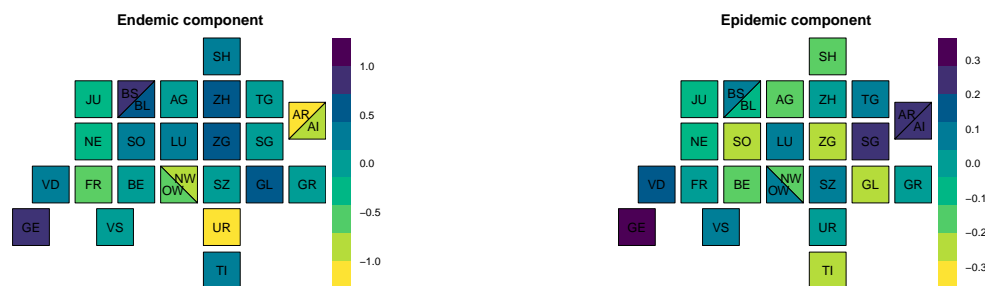


Figure 9: Estimated random effects of region in endemic-epidemic model with time-varying transmission weights and vaccination coverage in the endemic component

246 4.3 Scenario prediction

247 In the alternative scenario with more vaccines given throughout Switzerland (all re-
 248 gions get the maximum amount given for any region r at each time point), we would ex-
 249 pect a lower mean incidence in Zurich (ZH), the most populous region which often had
 250 the greatest vaccination uptake (Figure 5). We find that regions with lower vaccination
 251 coverage such as Glarus (GL), Appenzell Innerrhoden (AI), and Sankt Gallen (SG) have a
 252 greater drop in cases under a scenario of increased uptake of vaccination (see the support-
 253 ing information (file models-regions) for regional prediction plots) in ISO weeks 2021-30
 254 and 2021-38. Overall less cases would be expected if more vaccines had been distributed
 255 (Figure 10).

256 We also see that the age-based distribution scheme is evident in the comparison with
 257 an alternative as the greatest expected increases initially are among those groups vacci-
 258 nated first; over 65 year olds. We see an overall decrease in expected cases for younger age
 259 groups. The age group 50 – 59 is the youngest group to not only experience decreases but
 260 first see an increase then a decrease. This occurs at different times (ISO week 2021-34 for
 261 50 – 59, 2021-37 for 60 – 69, and 2021-38 for 70 – 79 and 80+) but after week 2021-
 262 38 all age groups would be expected to have fewer cases (see the supporting information
 263 (file models-age) for prediction plots by age group). On average, an increase would be
 264 expected but at the end of the study period less cases would be expected. A distribution
 265 scheme which is more uniform across age groups leads to predicted proportions of cases

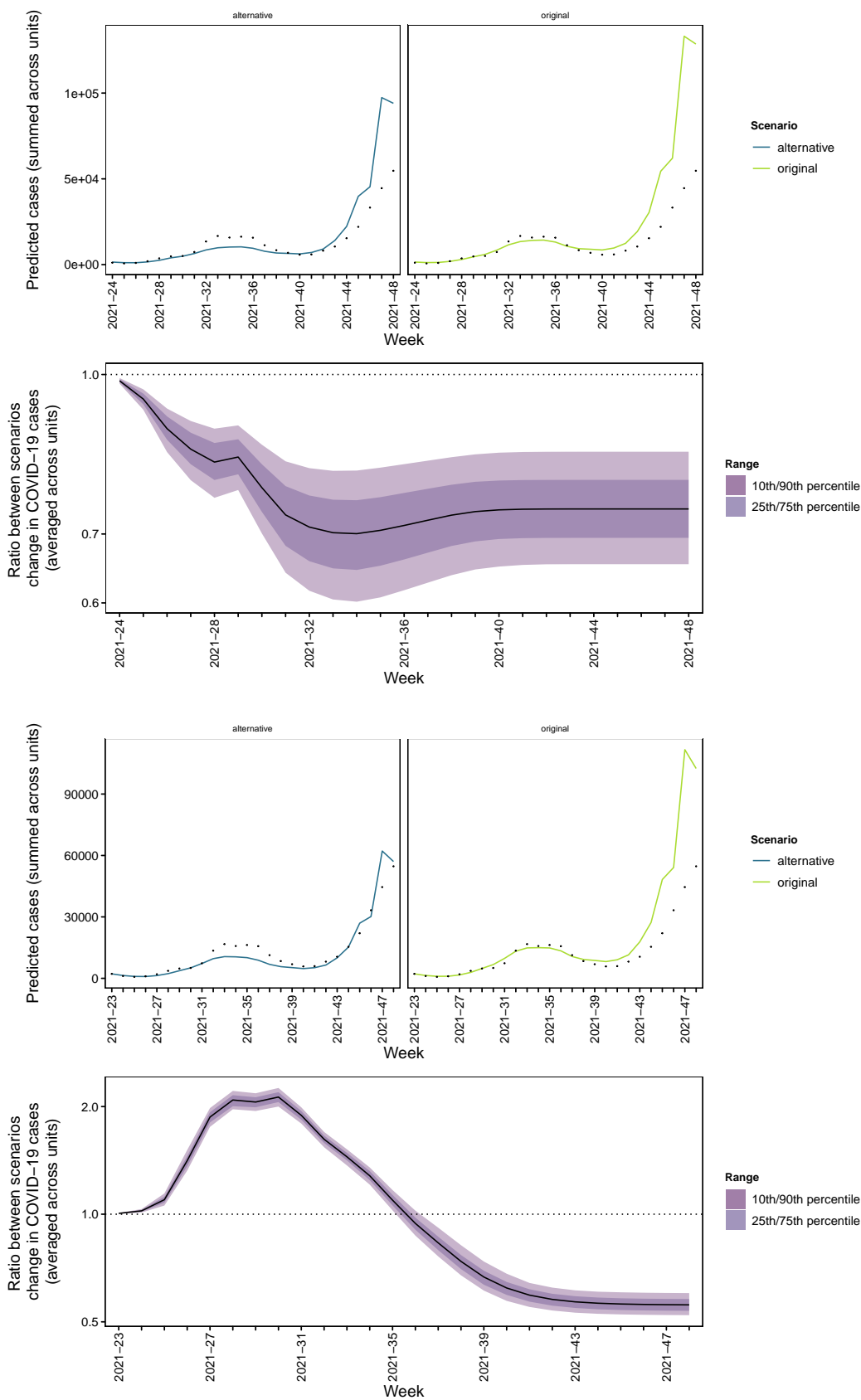


Figure 10: Predicted cases under the two alternative vaccination strategies for regions (above) and age groups (below)

266 being more equal (see supporting information (file supp) for plot), as would be expected.

267 **5 Conclusion**

268 This is the first use of endemic-epidemic modelling with time-varying transmission
269 weights and time-varying vaccination coverage concurrently. The vaccination coverage is
270 constructed in such a manner that is also takes into account waning immunity. The meth-
271 ods chosen for this work are relevant for case counts arising from a surveillance system for
272 notifiable diseases and so are useful for researchers and public health agency staff who in-
273 teract with such systems daily. The use of these models enable us to explore public health-
274 related questions and concerns using statistically sound methodology.

275 This work complements our earlier work on time-varying weights in endemic-epidemic
276 models [see 5–7]. The question for infectious disease models with transmission weight ma-
277 trices has always been and remains how do you choose which matrix to use. Replacing
278 who-acquires-infection-from-whom matrices with empirical or synthetic contact matrices
279 provided freedom from making assumptions of specific mixing patterns. However, during
280 a public health emergency such as COVID-19, assumptions of constant transmission op-
281 portunities may be violated due to disease control measures enacted. In such a setting the
282 choice of a constant matrix becomes non-trivial as non-outbreak settings (where surveys
283 of transmission opportunities are traditionally conducted) may no longer be representative
284 at short or long term scale and is is not obvious what should be chosen in such a setting.
285 For this reason, we adjusted the matrices to reflect situational changes using external in-
286 formation (policy and mobility). This does not fully answer the question but is an attempt
287 at determining which transmission weight matrices to use. As the changes to different con-
288 tact settings are not as obvious as in previous work [see 6, 7, and note the two flat lines
289 in the bottom left panel in Figure 1], we effectively only have changes to contacts driven
290 by specific locations. For other researchers wishing to do similar modelling, it should also
291 be noted that the mobility data informing m_{rt} is only made available until May 2022 after
292 which time it is no longer provided. This is an example of why private corporations should
293 not be in charge of data gathering for emergency response—access or collection can and

294 may be revoked at any time. In constructing such scenarios, we did not consider the sit-
295 uation of no vaccination as examined by Zwahlen and Staub [27] in their considerations
296 of expected excess deaths in the absence of vaccines. As they note, an endemic situation
297 with no vaccines and no disease control in place is unlikely. We would thus expect to see
298 certain contrasting effects in the time-varying transmission weights and the time-varying
299 vaccination coverage.

300 We showed that the endemic-epidemic modelling framework can be used to project the
301 COVID-19 pandemic under different scenarios of vaccination coverage. This was possible
302 as we worked with highly structured vaccine coverage data (which was stratified by week,
303 age group, and region). The objective of this project was to determine the role of vaccines
304 in slowing the spread of COVID-19 in Switzerland incorporating the specific demographics
305 of the country to improve the understanding of the impact of vaccination on the ongoing
306 pandemic. Statistical modelling was used with epidemiological data to determine the effect
307 unvaccinated or under-vaccinated groups have on the spread of COVID-19 in other parts of
308 Switzerland as well as the impact of the vaccination strategy used (age-based distribution).

309 The strength of our modelling work is the ability to project the epidemic under dif-
310 ferent scenarios for vaccination coverage taking into account waning. The highly struc-
311 tured case and vaccine data (given by weeks t , age group a , and region r) allows us to
312 obtain multivariate predictions providing stratified mean incidence. This is uniquely in-
313 formative and provides granular estimates of changes in numbers of cases. An alterna-
314 tive approach which would not allow for the evaluation of the vaccination coverage effect
315 estimate (which was the focus of this work) but which could be used to examine similar
316 research questions as considered here would be to inform the time-varying transmission
317 weights by the level of vaccination coverage. We have not considered such an approach
318 in this work as it is out of scope but mention it should other researchers wish to attempt
319 it. Meyer et al. [26] note that when you assume a common intercept for the unit, you do
320 not have to exclude units without reported cases. This should not be an issue here based
321 on visual inspection of the outcome variable data. Later developments [12] have examined
322 how to incorporate low case counts in endemic-epidemic models and may be another op-

323 tion to consider for researchers interested in similar questions.

324 We used the log-proportion of the unvaccinated population to represent the susceptible
325 population. This is based in the law of mass action which relies on a homogeneous mix-
326 ing assumption. We believe that our inclusion of time-varying heterogeneous contact and
327 spatial dispersion matrices as well as allowing the vaccination coverage to vary over time
328 relaxes some of the unrealistic aspects of such an assumption. Our work implicitly assumed
329 that in the scenarios of increased uptake of vaccines the alternative amount of vaccine
330 would be available which might not be the case in reality and so we note that our work
331 provides optimistic estimates. Because the Swiss national identity is very divided (Switzer-
332 land itself has notable linguistic divisions), it is perhaps not so surprising that Ticino (TI)
333 had early uptake of vaccines (Figure 3.2) as those residents would all other things equal
334 be assumed to have read more of the Italian language reporting on COVID-19; Italy being
335 the early European epicentre in 2022 could have had an impact. However, Rudolf Steiner-
336 based initiatives are head-quartered in Switzerland (particularly in Solothun (SO) which
337 never achieves the maximum vaccination coverage in the study period) and are known to
338 harbour pseudo-scientific and anti-vaccination sentiments [1] which could serve as a hin-
339 drance to improvements in vaccination and health. Waldorf school-driven outbreaks of
340 infectious diseases are a known epidemiologic issue [28]. With even more granular infor-
341 mation, the effects of undervaccinated school districts could be explored.

342 Much has been discussed about herd immunity during the COVID-19 pandemic after
343 the introduction of vaccines. Herd immunity is the proportion of population that needs to
344 be vaccinated in order to curb disease spread. The modelling approach used here can in
345 future also be used to examine the effects of achieving herd immunity, once this threshold
346 has been fully determined for this disease.

347 **ORCID**

348 M. Bekker-Nielsen Dunbar (0000-0002-7249-3524)

349 L. Held (0000-0002-8686-5325)

350 Declaration of interest

351 The authors declare no conflicts of interest or competing interests.

352 Reproducibility

353 Our analysis is fully reproducible using the code available at [github.com/mariabnd/](https://github.com/mariabnd/ee-vax)
354 [ee-vax](https://github.com/mariabnd/ee-vax). This includes a script which downloads the input data used in the analysis as well
355 as scripts we used for pre-processing this data. Our derived data is also released to safe-
356 guard for the future; the derived data will remain available even when the input data may
357 not longer be accessible. The code used in the documents (manuscript and supporting in-
358 formation) is also provided such that users can reproduce figures should they wish to.

359 References

- 360 [1] S. H. van Wees, K. Abunnaja, and S. Mounier-Jack. Understanding and explaining
361 the link between anthroposophy and vaccine hesitancy: A systematic review. 2022.
362 DOI:[10.21203/rs.3.rs-2208907](https://doi.org/10.21203/rs.3.rs-2208907).
- 363 [2] M. J. Deml, K. Jafflin, S. Merten, B. Huber, A. Buhl, E. Frau, V. Mettraux, J. Son-
364 deregger, P. Kliem, R. Cattalani, D. Krüerke, C. Pfeiffer, C. Burton-Jeangros,
365 and P. E. Tarr. Determinants of vaccine hesitancy in Switzerland: study proto-
366 col of a mixed-methods national research programme. *BMJ Open*, 9(11), 2019.
367 DOI:[10.1136/bmjopen-2019-032218](https://doi.org/10.1136/bmjopen-2019-032218).
- 368 [3] D. Kirton. 'I don't trust it:' Vaccine hesitancy lingers even as China COVID cases
369 surge. 2022. URL [https://www.reuters.com/world/china/i-dont-trust-it-
370 vaccine-hesitancy-lingers-even-china-covid-cases-surge-2022-12-19/](https://www.reuters.com/world/china/i-dont-trust-it-vaccine-hesitancy-lingers-even-china-covid-cases-surge-2022-12-19/).
- 371 [4] C. Veys-Takeuchi, S. Gonseth Nusslé, S. Estoppey, C. Zuppinger, J. Dupraz,
372 J. Pasquier, V. Faivre, R. Scuderi, S. Vassaux, M. Bochud, and V. D'Acromont. De-
373 terminants of COVID-19 vaccine hesitancy during the pandemic: A cross-sectional

- 374 survey in the canton of Vaud, Switzerland. *International Journal of Public Health*, 67,
375 2022. DOI:[10.3389/ijph.2022.1604987](https://doi.org/10.3389/ijph.2022.1604987).
- 376 [5] M. Grimée, M. Bekker-Nielsen Dunbar (joint first authors), F. Hofmann, and L. Held.
377 Modelling the effect of a border closure between Switzerland and Italy on the spa-
378 tiotemporal spread of COVID-19 in Switzerland. *Spatial Statistics*, page 100552,
379 2021. DOI:[10.1016/j.spasta.2021.100552](https://doi.org/10.1016/j.spasta.2021.100552).
- 380 [6] M. Bekker-Nielsen Dunbar, F. Hoffmann, and L. Held. Assessing the effect of school
381 closures on the spread of COVID-19 in Zurich. *Journal of the Royal Statistical Society*
382 *Series A*, 2022. DOI:[10.1111/rssa.12910](https://doi.org/10.1111/rssa.12910).
- 383 [7] M. Bekker-Nielsen Dunbar, F. Hofmann, S. Meyer, and L. Held (joint last authors).
384 Endemic-epidemic modelling of school closure to prevent spread of COVID-19 in
385 Switzerland (protocol available at DOI:[10.17605/osf.io/qh3gd](https://doi.org/10.17605/osf.io/qh3gd)). *medRxiv*, 2023.
386 DOI:[10.1101/2023.03.21.23287519](https://doi.org/10.1101/2023.03.21.23287519).
- 387 [8] M. Bekker-Nielsen Dunbar and L. Held. STUDY PROTOCOL: The COVID-19 vac-
388 cination campaign in Switzerland and its impact on disease spread. *Open Science*
389 *Foundation*, 2022. DOI:[10.17605/OSF.IO/6X4VK](https://doi.org/10.17605/OSF.IO/6X4VK).
- 390 [9] S. A. Herzog, M. Paul, and L. Held. Heterogeneity in vaccination coverage explains
391 the size and occurrence of measles epidemics in German surveillance data. *Epidemiol-*
392 *ogy & Infection*, 139(4):505–515, 2011. DOI:[10.1017/S0950268810001664](https://doi.org/10.1017/S0950268810001664).
- 393 [10] A. Robert, A. J. Kucharski, and S. Funk. The impact of local vaccine coverage and
394 recent incidence on measles transmission in France between 2009 and 2018. *BMC*
395 *Medicine*, 20(1):77, 2022. DOI:[10.1186/s12916-022-02277-5](https://doi.org/10.1186/s12916-022-02277-5).
- 396 [11] T. H. T. Nguyen, T. V. Nguyen, Q. C. Luong, T. V. Ho, C. Faes, and N. Hens. Un-
397 derstanding the transmission dynamics of a large-scale measles outbreak in south-
398 ern Vietnam. *International Journal of Infectious Diseases*, 122:1009–1017, 2022.
399 DOI:[10.1016/j.ijid.2022.07.055](https://doi.org/10.1016/j.ijid.2022.07.055).

- 400 [12] J. Lu and S. Meyer. A zero-inflated endemic-epidemic model with an application to
401 measles time series in Germany. *arXiv*, 2022. DOI:[10.48550/arxiv.2201.07285](https://doi.org/10.48550/arxiv.2201.07285).
- 402 [13] S.-E. Mamelund, C. Shelley-Egan, and O. Rogeberg. The association between socioe-
403 conomic status and pandemic influenza: Systematic review and meta-analysis. *PLOS*
404 *ONE*, 16(9):1–31, 2021. DOI:[10.1371/journal.pone.0244346](https://doi.org/10.1371/journal.pone.0244346).
- 405 [14] D. Mistry, M. Litvinova, A. Pastore y Piontti, M. Chinazzi, L. Fumanelli, M. F. C.
406 Gomes, S. A. Haque, Q.-H. Liu, K. Mu, X. Xiong, M. E. Halloran, I. M. Longini,
407 S. Merler, M. Ajelli, and A. Vespignani. Inferring high-resolution human mix-
408 ing patterns for disease modeling. *Nature Communications*, 12(1), 2021.
409 DOI:[10.1038/s41467-020-20544-y](https://doi.org/10.1038/s41467-020-20544-y).
- 410 [15] T. Hale, N. Angrist, R. Goldszmidt, B. Kira, A. Petherick, T. Phillips, S. Webster,
411 E. Cameron-Blake, L. Hallas, S. Majumdar, and H. Tatlow. A global panel database
412 of pandemic policies (Oxford COVID-19 Government Response Tracker). *Nature Hu-*
413 *man Behaviour*, 5(4):529–538, 2021. DOI:[10.1038/s41562-021-01079-8](https://doi.org/10.1038/s41562-021-01079-8).
- 414 [16] EBG. A tilemap for Switzerland. 2016. URL [https://github.com/ebp-group/
415 Switzerland_Tilemap](https://github.com/ebp-group/Switzerland_Tilemap).
- 416 [17] S. Meyer, L. Held, and M. Høhle. Spatio-temporal analysis of epidemic phenomena
417 using the R package surveillance. *Journal of Statistical Software*, 77(11):1–55, 2017.
418 DOI:[10.18637/jss.v077.i11](https://doi.org/10.18637/jss.v077.i11).
- 419 [18] L. Held, M. Höhle, and M. Hofmann. A statistical framework for the analysis of mul-
420 tivariate infectious disease surveillance counts. *Statistical Modelling*, 5(3):187–199,
421 2005. DOI:[10.1191/1471082X05st098oa](https://doi.org/10.1191/1471082X05st098oa).
- 422 [19] M. Paul and L. Held. Predictive assessment of a non-linear random effects model for
423 multivariate time series of infectious disease counts. *Statistics in Medicine*, 30(10):
424 1118–1136, 2011. DOI:[10.1002/sim.4177](https://doi.org/10.1002/sim.4177).

- 425 [20] L. Held and M. Paul. Modeling seasonality in space-time infectious
426 disease surveillance data. *Biometrical Journal*, 54(6):824–843, 2012.
427 DOI:[10.1002/bimj.201200037](https://doi.org/10.1002/bimj.201200037).
- 428 [21] S. Meyer and L. Held. Incorporating social contact data in spatio-temporal
429 models for infectious disease spread. *Biostatistics*, 18(2):338–351, 2016.
430 DOI:[10.1093/biostatistics/kxw051](https://doi.org/10.1093/biostatistics/kxw051).
- 431 [22] S. Meyer and L. Held. Power-law models for infectious disease spread. *Annals of*
432 *Applied Statistics*, 8:1612–1639, 2014. DOI:[10.1214/14-AOAS743](https://doi.org/10.1214/14-AOAS743).
- 433 [23] L. Held, S. Meyer, and J. Bracher. Probabilistic forecasting in infectious disease epi-
434 demiology: the 13th Armitage lecture. *Statistics in Medicine*, 36(22):3443–3460,
435 2017. DOI:[10.1002/sim.7363](https://doi.org/10.1002/sim.7363).
- 436 [24] Y. Xia, O. N. Bjørnstad, B. T. Grenfell, and D. L. DeAngelis. Measles metapopulation
437 dynamics: A gravity model for epidemiological coupling and dynamics. *American*
438 *Naturalist*, 164(2):267–281, 2004. DOI:[10.1086/422341](https://doi.org/10.1086/422341).
- 439 [25] S. den Boon, M. Jit, M. Brisson, G. Medley, P. Beutels, R. White, S. Flasche,
440 T. D. Hollingsworth, T. Garske, V. E. Pitzer, M. Hoogendoorn, O. Geffen, A. Clark,
441 J. Kim, and R. Hutubessy. Guidelines for multi-model comparisons of the im-
442 pact of infectious disease interventions. *BMC Medicine*, 17(1):163, 2019.
443 DOI:[10.1186/s12916-019-1403-9](https://doi.org/10.1186/s12916-019-1403-9).
- 444 [26] S. Meyer, L. Held, and M. Höhle. Spatio-temporal analysis of epidemic phenomena
445 using the R package surveillance. *Journal of Statistical Software*, 77(11):1–55, 2017.
446 DOI:[10.18637/jss.v077.i11](https://doi.org/10.18637/jss.v077.i11).
- 447 [27] M. Zwahlen and K. Staub. What would have happened if we would not have had the
448 COVID vaccination? *Swiss Medical Weekly*, 2022. URL [https://smw.ch/op-eds/
449 post/what-would-have-happened-if-we-would-not-have-had-the-covid-
450 vaccination-could-the-pandemic-death-toll-2020-2021-have-reached-
451 the-dimensions-of-the-1918-1919-pandemic](https://smw.ch/op-eds/post/what-would-have-happened-if-we-would-not-have-had-the-covid-vaccination-could-the-pandemic-death-toll-2020-2021-have-reached-the-dimensions-of-the-1918-1919-pandemic).

452 [28] E. Ernst. Anthroposophy: A risk factor for noncompliance with measles im-
453 munization. *Pediatric Infectious Disease Journal*, 30(3):187–189, 2011.
454 DOI:[10.1097/INF.0b013e3182024274](https://doi.org/10.1097/INF.0b013e3182024274).